JOURNAL OF SEPARATION SCIENCE

22|2021
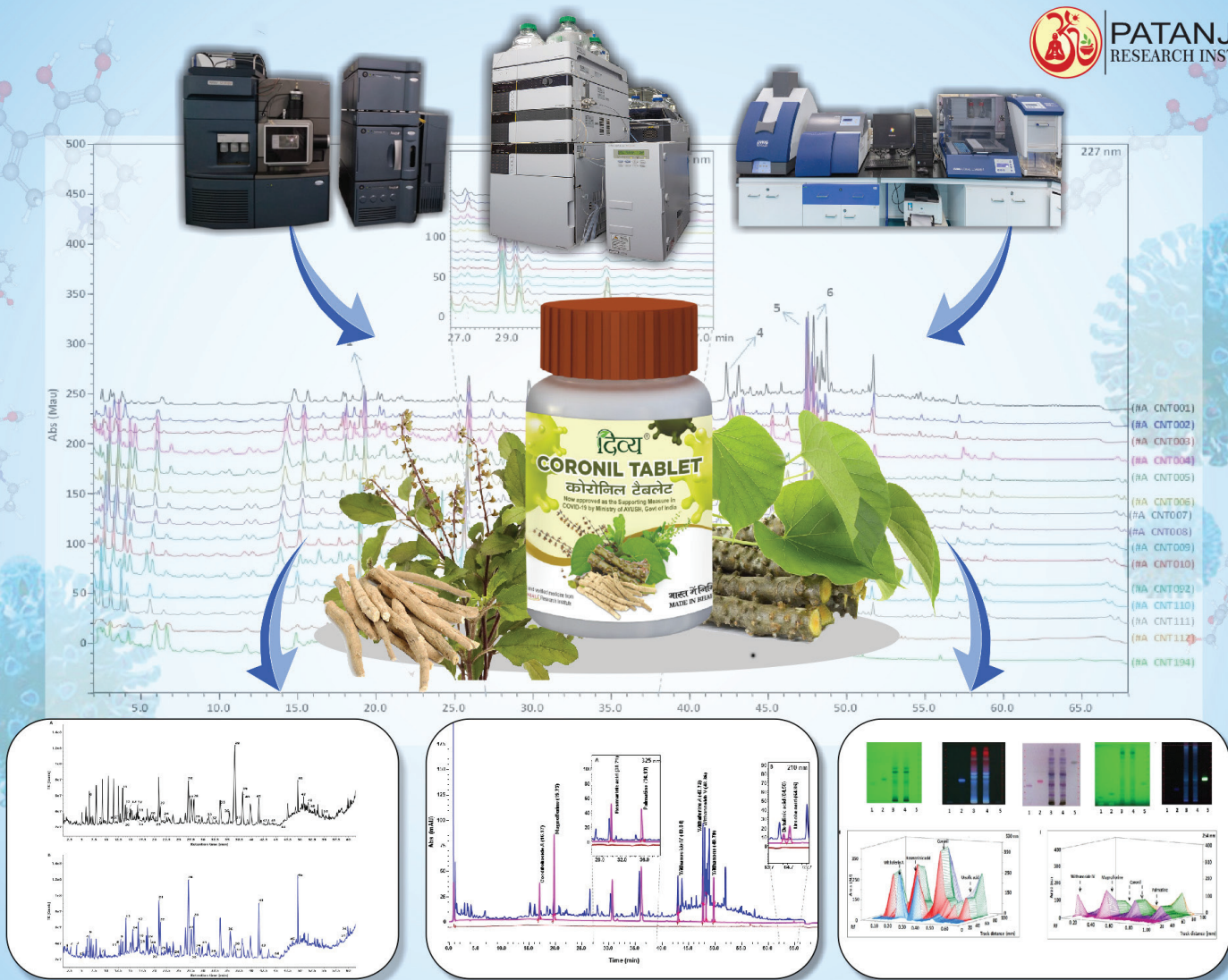
PATANJALI
RESEARCH INSTITUTE

RESEARCH ARTICLE

JOURNAL OF
SEPARATION SCIENCE

Phytometabolite profiling of Coronil, a herbal medicine for COVID-19, its identification by mass-spectroscopy and quality validation on liquid chromatographic platforms

Acharya Balkrishna[1,2] | Meenu Tomer[1] | Sudeep Verma[1] | Monali Joshi[1] | Priyanka Sharma[1] | Jyotish Srivastava[1] | Anurag Varshney[1,2,3] 🔘

[1] Drug Discovery and Development Division, Patanjali Research Institute, NH-58, Haridwar, Uttarakhand 249405, India

[2] Department of Allied and Applied Sciences, University of Patanjali, Patanjali Yogpeeth, NH-58, Haridwar, Uttarakhand 249405, India

[3] Special Centre for Systems Medicine, Jawaharlal Nehru University, New Delhi 110067, India

Correspondence
Dr. Anurag Varshney, Drug Discovery and Development Division, Patanjali Research Institute, NH-58, Haridwar 249 405, Uttarakhand, India.
Email: anurag@prft.co.in

Funding information
Patanjali Research Foundation Trust, Haridwar, India

Coronil is a tri-herbal medicine consisting of immunomodulatory herbs, *Withania somnifera*, *Tinospora cordifolia*, and *Ocimum sanctum*. The formulation has been developed specifically as the supporting measure for COVID-19. Current investigation is aimed to identify the phytoconstituents in Coronil utilizing ultra-performance liquid chromatography–mass spectrometry coupled with quadrupole time of flight and to establish its quality standardization using high-performance liquid chromatography and high performance thin layer chromatography. Out of 52 identified compounds, cordifolioside A, magnoflorine, rosmarinic acid, palmatine, withanoside IV, withanoside V, withanone, betulinic acid, and ursolic acid were quantified in 15 different batches of Coronil on validated high-performance liquid chromatography method. Similarly, withanoside IV, withaferin A, magnoflorine, palmatine, rosmarinic acid, and ursolic acid were analyzed on high performance thin layer chromatography. Methods were validated as per the International Council for Harmonization guidelines. These methods were specific, reproducible, accurate, precise, linear ($r^2 > 0.99$), and percent recoveries were within the prescribed limits. The content uniformity of Coronil was ascertained using Fourier transform infrared spectroscopy. Results indicated that, validated methods were fit for their intended use and the analytical quality of Coronil was consistent across the batches. Taken together, these developed methods could drive the analytical quality control of herbal medicines such as Coronil, and other formulations containing similar chemical profiles.

KEYWORDS
ayurveda, Coronil, liquid chromatography, mass spectrometry, validation

---

Nonstandard Abbreviations: RBD, receptor binding domain; SARS-CoV-2, Severe Acute Respiratory Syndrome Coronavirus 2

1 | INTRODUCTION

The pandemic of novel coronavirus disease (COVID-19) caused by Severe Acute Respiratory Syndrome Coronavirus 2 (SARS-CoV-2) is unique and unprecedented in several aspects. It has opened the battlefront in healthcare systems across the globe [1]. Despite worldwide efforts to contain it, the pandemic has been continuing to spread. This demands for clinically proven prophylaxis and therapeutic strategies without any harmful aftermaths to the human race [2]. Thus, at a time of this worldwide anxiety, dimensions of pandemic demand imperative long-term solutions of all knowledge systems available globally [3]. In India, several initiatives have been taken to utilize Ayurvedic therapies as a preventative measure against COVID-19. Drinking warm water all through the day and consumption of herbal tea are among a few of the suggested Ayurvedic therapies [4]. The crux of the matter is that prevention is better than cure. Ayurveda, one of the world-renowned forms of Indian traditional medicine, showcases a great deal of immunity-boosting therapies. Coronil is one such formulation, which is based on the trusted classical principles of Ayurveda. Coronil is a tri-herbal medicine enriched with the extracts of three potential antiviral and immunomodulatory herbs, *Tinospora cordifolia* (Saptaśirikā aromapatrā, Giloy, heart-leaved moonseed), *Withania somnifera* (Aśvagandhakaḥ svāpakaraḥ, Ashwagandha, winter cherry), and *Ocimum sanctum* (Sumañjarikā rāmā, Tulsi, holy basil). The Coronil formulation has emerged as the viable option for combating COVID-19 contagion.

Tinospora cordifolia holds a special position in Ayurvedic literature for its diverse therapeutic application. The major phytocomponents reported in this medicinal plant are cordifolioside A, magnoflorine, tinocordiside, palmatine, and syringin. Metabolites of this herb have been reported to possess immune-boosting properties [5]. The antiviral potential of the palmatine alkaloid has been established against the main protease complex (Mpro) of SARS-CoV-2 [6]. *Ocimum sanctum* is often referred to as an "elixir of life" for its vast array of medicinal properties [7]. Pharmacologically, *O. sanctum* has been explored in hundreds of scientific studies including in vitro, animal and human experiments. Experimental evidences have also demonstrated that selected naturally occurring compounds from *O. sanctum* exhibit antiviral activities [8]. In same line, Wen and co-workers evaluated betulinic acid, one of the *O. sanctum* compound, for its anti-SARS-CoV activity in Vero-E6 cells on a cell-based cytopathic effect assay [9]. The compounds such as ursolic acid, carnosol, rosmarinic acid, cirsilineol, apigenin, eugenol, and

cirsimaritin present in *O. sanctum* upregulate IL-2 and IFN-ϒ, and downregulate IL-1β, which represent a major defense mechanism to assess T-cell-dependent antibody responses [10]. *Withania somnifera* has been considered with a combination of versatile immunomodulatory phytoconstituents. Compounds of *W. somnifera*, Withaferin A and withanone, have been shown to significantly block the entry of SARS-CoV-2 in host cells [11]. Pathophysiology of SARS-CoV-2 indicates that the virus invades the host cell receptor angiotensin-converting enzyme 2 (ACE2) through its spike protein receptor binding domain (RBD). Withanone and tinocordiside docked very well in the binding interface of ACE2-RBD complex and significantly attenuated the electrostatic component of binding free energies of ACE2–RBD complex [12,13]. Docking result postulates that natural phytochemicals indeed have the potential to fight against COVID-19 and its pathogenicity. With this rationality, innate potentials of *W. somnifera*, *T. cordifolia*, and *O. sanctum* are utilized to formulate "Coronil" (referred as CNT now onwards), as an effective pharmaceutical agent to combat SARS-CoV-2 infectivity [14,15].

To assure the safety and efficacy of these traditional medicines, it is critical to establish their comprehensive qualitative assessment methods [16]. The key ingredients of CNT constitute a plethora of bioactive secondary metabolites, which makes the simultaneous determination of active ingredients necessary for its comprehensive quality evaluation.

This encouraged us to develop rapid, sensitive, and reliable analytical methods using RP-HPLC with photo diode array detector (RP-HPLC-PDA), high performance thin layer chromatography (HPTLC), and FTIR spectroscopy as strategic tools for the CNT quality assessment. UHPLC/MS coupled with quadrapole TOF (UHPLC/MS-ToF) analyzer is one of the foremost effective techniques for ionizable moieties with high mass precision [17]. The CNT analytical evaluation was initiated by screening of potential biomarkers utilizing UHPLC/MS-ToF platform. For CNT, selected markers, rosmarinic acid, magnoflorine, palmatine, withaferin A, withanoside IV, withanoside V, cordifolioside, betulinic acid, withanone, and ursolic acid were quantified simultaneously, by utilizing the developed and validated RP-HPLC-PDA and HPTLC techniques for the first time. The stability of the formulation was also evaluated under different solvents, temperature, and light conditions. The developed RP-HPLC-PDA method was then utilized for the quantification of the target compounds in 15 different batches of CNT. Moreover, FTIR fingerprinting was performed to ascertain batch-to-batch consistency of CNT formulation.

2 | MATERIALS AND METHODS

2.1 | Chemicals, reagents, and samples

The HPLC and LCMS grade solvents acetonitrile and methanol were obtained from E-Merck and Honeywell (Germany), respectively. Analytical grade solvents, glacial acetic acid, and formic acid were procured from Honeywell, Germany; p-anisaldehyde, sulphuric acid, toluene, and ethyl acetate were purchased from E-Merck, Germany. Deionized water, purified by a Milli-Q system (Millipore, USA), was used throughout the study. Standards, Palmatine hydrochloride (cat #361615), Magnoflorine (cat #361615), and Rosmarinic acid (cat #R4033), were procured from Sigma Aldrich, USA. Ursolic acid (cat #102067769, Tokyo chemical industries, Japan) and Cordifolioside A (cat #CFN95040, Chemfaces, China), were also used in the study. Betulinic acid (cat #B2836), Withanone (cat #W005), Withaferin A (cat #W003), Withanoside IV (cat #W006), and Withanoside V (cat #W007) were sourced from Natural Remedies, India for analysis. CNT samples, from the batch #ACNT 001 were used for the RP-HPLC studies. Whereas, CNT batch #ACNT 002 was taken into consideration for the UPLC/MS-ToF and HPTLC analysis. Quantitative analysis was performed on 15 different batches (#ACNT 001 to 010, 092, 110 to 112, and 194) whereas stability studies were performed on the batches (#ACNT 194, 009, and 460). CNT samples were sourced from Divya Pharmacy, Haridwar, India, and were stored in airtight bottles for further use.

2.2 | Analytical investigations

2.2.1 | Ultra high performance liquid chromatography–mass spectrometry coupled with quadrapole time of flight analysis

Preparation of Coronil sample solution
10 mL of methanol:water (80:20) was added to 100 mg of powdered CNT sample and sonicated for 15 min. The solution was then centrifuged for 5 min at 5000 rpm and filtered using a 0.22 μm nylon filter. The filtered solution was used for the analysis.

Instrumentation
The analysis was performed on a Xevo G2-XS QToF Waters Corporation (MA, USA) with Acquity UPLC I-Class and Unifi software (Waters Corporation, USA). The separation was carried out using Nucleodur C18 Gravity column (100 × 2.0 mm, 1.8 μm) (Macherey-Nagel, USA). The column was maintained at 35°C and the sample temperature was kept at 20°C during the

analysis. The main working parameters for MS were: ionization type-ESI, mode-MS^E, acquisition time 62 min, mass range (m/z) 50−1200 m/z, low collision energy 6 eV, high collision energy 20−40 eV (ramp), cone voltage 40 V, capillary voltage 1.5 kV (for positive mode), 2 kV (for negative mode), source temperature 120°C, desolvation temperature 500°C, cone gas flow 50 L/h, desolvation gas flow 900 L/h. Mass was corrected during acquisition, using an external reference (Lock–Spray) consisting of 0.2 ng/mL solution of leucine enkephalin (Waters , USA) infused at a flow rate of 10 μL/min via a lock–spray interface, generating a reference ion for the positive ion mode [(M+H) m/z 556.2766] and for the negative ion mode [(M-H) m/z 554.2620] to ensure mass correction during the MS analysis. The Lock–Spray scan time was set at 0.25 s with an interval of 30 s. The elution was carried out at a flow rate of 0.3 ml/min using gradient mobile phase, 0.1% formic acid in water (solvent A), and 0.1% formic acid in acetonitrile (solvent B). The volume ratio of solvent B was changed as follows, 5–10% B for 0–5 min, 10–20% B for 5–15 min, 20–30% B for 15–35 min, 30–35% B for 35–45 min, 35–80% B for 45–60 min, 80–90% B for 60–65 min, 90–5% B for 65–66 min, and 5% B for 66–70 min. 2 μL of the test solution was injected for the screening and the chromatographs were recorded for 62 min.

Identification of marker components in Coronil
The marker components in CNT were identified and affirmed by their respective mass ion, fragmentation pattern, offline and online mass spectral database, and related literature. Data acquisitions were executed under positive (+ve) and negative (−ve) mode of ionization utilizing full spectrum scan.

2.2.2 | HPLC and high performance thin layer chromatography method development and optimization

Preparation of standard solution
Stock solutions of cordifolioside A, magnoflorine, rosmarinic acid, palmatine, withanoside IV, withaferin A, withanoside V, withanone, betulinic, and ursolic acid (1000 ppm) were prepared by dissolving accurately weighed standards in methanol:water (80:20), to generate 50 ppm working standard solutions. For the HPTLC analysis, the stock solutions of reference standards were diluted using same solvent to prepare working standard solutions of 100 ppm for withanoside IV, withaferin A, rosmarinic acid, and ursolic acid. Whereas, 20 and 5 ppm standard solutions were prepared for magnoflorine and palmatine, respectively.

Preparation of Coronil sample solution
0.5 g of powdered CNT (batch #ACNT 001) was added to 10 ml methanol:water (80:20) and sonicated for 30 min. The sonicated solution was centrifuged for 5 min at 10 000 rpm and filtered through a 0.45 μm nylon filter and used for the analysis of cordifolioside A, magnoflorine, rosmarinic acid, palmatine, withanoside IV, withaferin A, withanoside V, withanone, betulinic, and ursolic acid. For HPTLC analysis, 0.5 g of CNT sample (batch #A CNT 002) was added with 5 ml of same diluent. The solution was sonicated for 30 min, centrifuged for 5 min at 10 000 rpm and filtered through a 0.45 μm nylon filter for the investigations of withanoside IV, withaferin A, magnoflorine, palmatine, rosmarinic acid, and ursolic acid.

Instrumentation and chromatographic conditions for HPLC
RP-HPLC-PDA analysis was performed on Prominence-XR HPLC system (Shimadzu, Japan) equipped with Quaternary pump (NexeraXR LC-20AD XR), PDA detector (SPD-M20 A), Auto-sampler (Nexera XR SIL-20 AC XR), Degassing unit (DGU-20A 5R), and Column oven (CTO-10 AS VP). A solvent system of water containing 0.1% orthophosphoric acid adjusted to pH 2.5 with diethylamine (solvent A) and acetonitrile (solvent B) was selected. Gradient elution program used during the analysis consisted of 5% B for 0−10 min, 5−15% B from 10−20 min, 15−25% B from 20−40 min, 25−65% B from 40−60 min, 65−90% B from 60−65 min, 90−5% B from 65−66 min, and 5% B from 66−70 min. The chromatograms acquired using a Shimadzu Shim pack, GIST-HP C18 (3 μm, 3 × 100 mm) (Shimadzu, Japan) with a flow rate of 0.7 ml/min. The chromatographic detection of all the analytes was performed using a PDA detector at 325, 227, and 210 nm. The temperature of the column was kept at 30°C and the sample injection volume was 5 μL.

Instrumentation and chromatographic conditions for high performance thin layer chromatography
High-performance TLC analysis was performed on CAMAG, (Muttenz, Switzerland) instrument and analyzed using silica gel 60F254 precoated with 15 μm silica (10 × 10 cm and 20 × 10 cm) HPTLC plates (Merck, CAT no: 1.05554.007, Mumbai, India). The samples were spotted in the form of bands, width 8 mm using the CAMAG Automated TLC Sampler 4 (ATS4), equipped with a 25 μl Hamilton syringe. The plates were developed in a previously saturated (15 min) CAMAG twin trough chamber (10 × 10 cm and 20 × 10 cm). The mobile phase consisted of toluene:ethyl acetate:formic acid (5:5:1), for withaferin A, rosmarinic acid, and ursolic acid. Ethyl acetate:formic acid:acetic acid:water (10:1.1:1.1:2.6) for withanoside IV,

palmatine, and magnoflorin, after development, plates were removed and dried using air dryer. For fingerprinting, the plates were visualized at 254, 366 nm, and under white light after derivatization using anisaldehyde sulfuric acid reagent (prepared by adding 1 mL of p-anisaldehyde in 70 mL methanol, 20 mL glacial acetic acid, and 10 ml of sulfuric acid. The prepared reagent was stored in an amber colored bottle). For visualization, the densitometric scanning was performed using TLC Scanner 4, with slit dimension (6.00 × 0.45 mm) and 20 mm/s scanning speed at the wavelengths of 530 nm for withaferin A, rosmarinic acid, and ursolic acid and 254 nm for withanoside IV, palmatine, and magnoflorine. For quantification, the plates were scanned at 230 nm for withaferin A, 265 nm for magnoflorine, 330 nm for palmatine, and rosmarinic acid. For ursolic acid, the developed plate was derivatized using anisaldehyde sulphuric acid and scanned at 530 nm.

2.2.3 | Fourier transform infrared spectroscopy analysis

The analysis was performed on Cary 630 FTIR (Agilent technologies, Malasyia) set at attenuated total reflection mode. Spectra were scanned over the frequency range of 650–4000 cm^{-1} with a spectral resolution of 16 cm^{-1}. For the spectrum acquisition, a powdered CNT sample from 15 different batches was placed onto the attenuated total reflection crystal.

2.3 | HPLC and high performance thin layer chromatography method validation

2.3.1 | HPLC

Ten marker components namely, cordifolioside A, magnoflorine, rosmarinic acid, palmatine, withanoside IV, withaferin A, withanoside V, withanone, betulinic, and ursolic acid were validated using RP-HPLC-PDA as per International Council on Harmonisation [ICH-Q2(R1)] guidelines [18]. System suitability was affirmed before the experimental analysis. The specificity of the developed method was evaluated by injecting 5 μL of the solvent blank (methanol:water, 80:20) at 325, 210, and 227 nm in both standard and sample matrices. Three-point peak purity of the analytes was considered to ensure the specificity of the developed method. For linearity, working standard solutions were prepared separately in different concentration ranges 0.25–100 μg/mL, by diluting the stock solution with methanol. The calibration curve was plotted between peak area and respective concentrations to
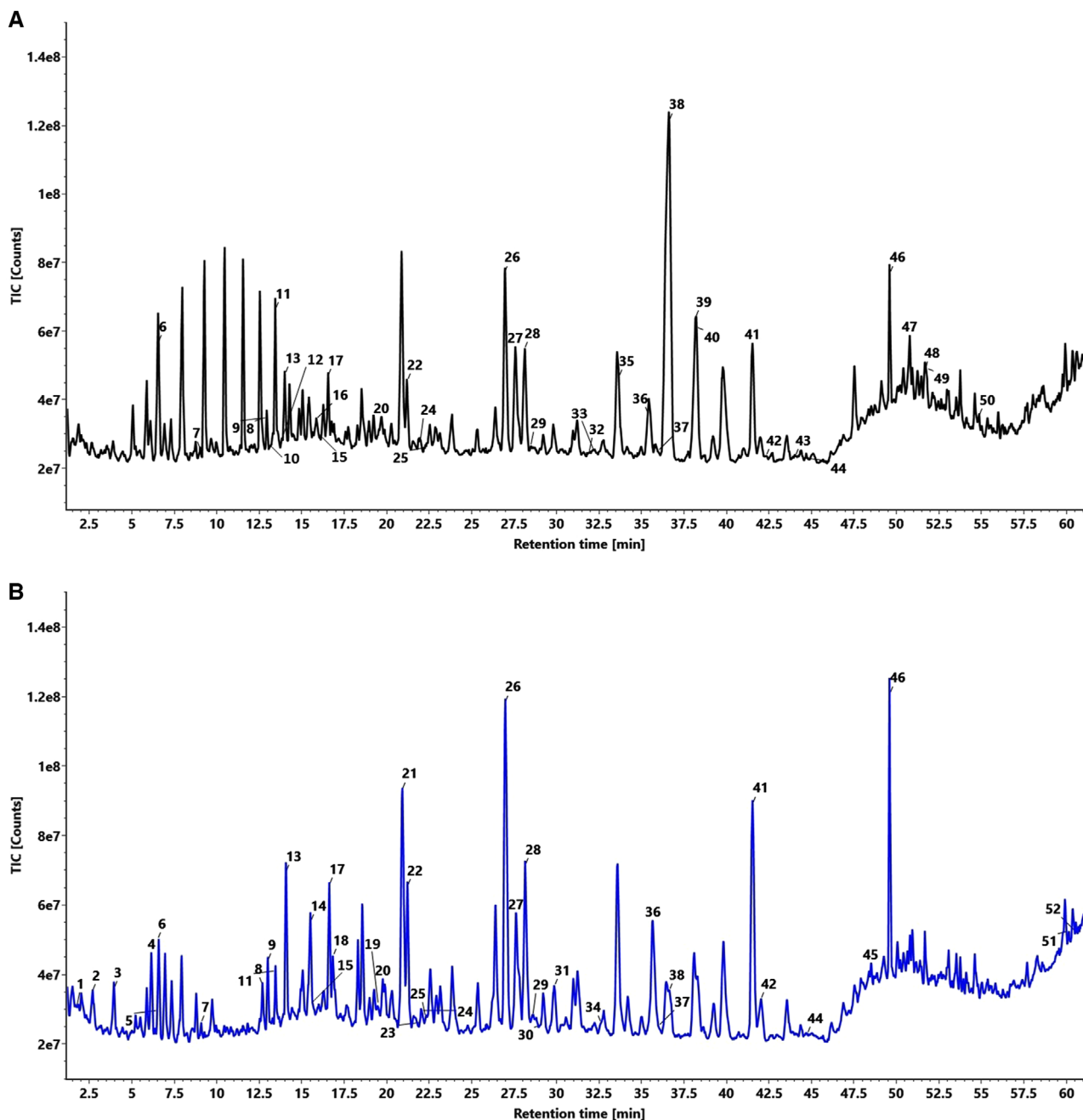
FIGURE 1 Total ion chromatogram of 52 compounds characterized in Coronil using UHPLC/MS-ToF in (A) positive mode (B) negative mode. Where, (1) gallic acid, (2) syringic acid, (3) neochlorgenic acid, (4) chlorogenic acid, (5) cordifolioside A, (6) magnoflorine, (7) kaempferol 3-O-rutinoside (nictoflorin), (8) rutin, (9) kaempferol-3-gentiobioside, (10) columbamine, (11) ecdysterone, (12) dihydroberberine, (13) luteolin-7-O-glucuronide, (14) rabdosiin, (15) astragalin, (16) palmatine, (17) apigenin 7-glucuronide, (18) rosmarinic acid, (19) tinosporide, (20) N-feruloyltyramine, (21) tinocordiside, (22) withanoside VIII (23) tanegoside, (24) quercetin (25) luteolin, (26) withanoside IV, (27) 3-HDH-withanolide F, (28) viscosalactone B, (29) kaempferol, (30) withanolide E, (31) physagulin D, (32) 2, 3-didehydrosomnifericin, (33) 3α, 6α-epoxy-4β, 5β,27-trihydroxy-1-oxowitha-24-enolide, (34) coagulin Q, (35) 24, 25-dihydrowithanolide D, (36) 2, 3-dihydro-3β-O-sulfate withaferin A, (37) 2, 3-dihydrowithaferin-A, (38) withaferin A, (39) quresimine, (40) crisilineol, (41) withanoside V, (42) withanone, (43) cirisimaritin, (44) methyl rosmarinate, (45) 12-deoxywithastramonolide, (46) ashwagandholide, (47) 5-hydroxy-7, 8-dimethoxyflavone, (48) 5-hydroxy-4′, 6, 7-trimethoxyflavone, (49) withanolide G, (50) dieugenol, (51) betulinic acid, and (52) ursolic acid were identified in Coronil formulation. See Table 1, and Supplementary Figures S1A to S1G for detailed information

TABLE 1 Identified metabolites in Coronil on UHPLC/QToF MS. See Figure 1, and Supplementary Figures S1A to S1G for detailed information

Peak no.	Component name	Formula	Neutral mass (Da)	Observed m/z	RT (min)	Mode	Fragments (m/z)
1	Gallic acid	$C_7H_6O_5$	170.0215	169.0126	1.74	−ve	$[C_7H_6O_5]^{-H}$, 125.0244, 123.0081
2	Syringic acid	$C_9H_{10}O_5$	198.0528	197.0433	2.67	−ve	$[C_9H_{10}O_5]^{-H}$, 179.0342, 150.0321, 135.0439, 134.0369, 123.0445
3	Neochlorogenic acid	$C_{16}H_{18}O_9$	354.0951	353.0839	3.93	−ve	$[C_{16}H_{18}O_9]^{-H}$, 191.0536, 179.0335, 173.0436, 135.0440, 134.0364
4	Chlorogenic acid	$C_{16}H_{18}O_9$	354.0951	353.0844	6.14	−ve	$[C_{16}H_{18}O_9]^{-H}$, 215.0534, 191.0540, 173.0437, 161.0231, 135.0441, 109.0290
5	Cordifolioside A	$C_{22}H_{32}O_{13}$	504.1843	549.1796	6.49	−ve	$[C_{22}H_{32}O_{13}]^{+HCOO}$, 381.1189, 167.0329, 121.0289
6	Magnoflorine	$C_{20}H_{23}NO_4$	341.1627	342.1704 340.1516	6.58 6.56	+ve −ve	$[C_{20}H_{23}NO_4]^{+H}$, 297.1117, 282.0883, 265.0855, 145.0268 $[C_{20}H_{23}NO_4]^{-H}$, 135.0440, 134.0364
7	Nictoflorin	$C_{27}H_{30}O_{15}$	594.1585	595.1659 593.1522	9.04 9.08	+ve −ve	$[C_{27}H_{30}O_{15}]^{+H}$, 577.1569, 541.1347, 457.1111, 379.0806, 355.0803, 270.0975, 243.0853, 137.0590 $[C_{27}H_{30}O_{15}]^{-H}$, 503.1174, 473.1061, 455.0959, 135.0443
8	Rutin	$C_{27}H_{30}O_{16}$	610.1534	611.1607 609.1478	12.64 12.70	+ve −ve	$[C_{27}H_{30}O_{16}]^{+H}$, 465.1016, 303.0494, 298.1062 $[C_{27}H_{30}O_{16}]^{-H}$, 151.0023
9	Kaempferol-3-gentiobioside	$C_{27}H_{30}O_{16}$	610.1534	611.1605 609.1485	12.96 13.01	+ve −ve	$[C_{27}H_{30}O_{16}]^{+H}$, 465.1018, 303.0495, 301.0692, 229.0485, 153.0171 $[C_{27}H_{30}O_{16}]^{-H}$, 463.0864, 311.0541, 191.0538, 151.0025
10	Columbamine	$C_{20}H_{19}NO_4$	337.1314	338.1385	13.32	+ve	$[C_{20}H_{19}NO_4]^{+H}$, 322.1065, 294.1115, 279.0880, 137.0590, 109.0276
11	Ecdysterone	$C_{27}H_{44}O_7$	480.3087	481.3149 525.3068	13.46 13.47	+ve −ve	$[C_{27}H_{44}O_7]^{+H}$, 445.2949, 427.2835, 409.2727, 371.2209, 353.2125, 265.1609, 191.1081, 165.1263 $[C_{27}H_{44}O_7]^{+HCOO}$, 461.2887, 159.1012
12	Dihydroberberine	$C_{20}H_{19}NO_4$	337.1314	338.1388	13.61	+ve	$[C_{20}H_{19}NO_4]^{+H}$, 322.1068, 294.1117, 279.0881, 145.0275, 117.0328
13	Luteolin-7-O-glucuronide	$C_{21}H_{18}O_{12}$	462.0798	463.0877 461.0708	14.01 14.09	+ve −ve	$[C_{21}H_{18}O_{12}]^{+H}$, 287.0548, 153.0174, 135.0432 $[C_{21}H_{18}O_{12}]^{-H}$, 133.0287
14	(−)-Rabdosiin	$C_{36}H_{30}O_{16}$	718.1534	717.1501	15.53	−ve	$[C_{36}H_{30}O_{16}]^{-H}$, 671.1414, 519.0931, 475.1014, 134.0356, 133.0287, 132.0211
15	Astragalin	$C_{21}H_{20}O_{11}$	448.1006	449.1082 447.0910	15.66 15.72	+ve −ve	$[C_{21}H_{20}O_{11}]^{+H}$, 287.0546 $[C_{21}H_{20}O_{11}]^{-H}$, 151.0024
16	Palmatine	$C_{21}H_{21}NO_4$	351.1471	352.1548	15.87	+ve	$[C_{21}H_{21}NO_4]^{+H}$, 336.1227, 308.1275, 294.1112
17	Apigenin 7-glucuronide	$C_{21}H_{18}O_{11}$	446.0849	447.0927 445.0753	16.56 16.64	+ve −ve	$[C_{21}H_{18}O_{11}]^{+H}$, 271.0597, 229.0486, 153.0173, 119.0484 $[C_{21}H_{18}O_{11}]^{-H}$, 175.0237, 151.0022, 113.0241
18	Rosmarinic acid	$C_{18}H_{16}O_8$	360.0845	359.0738	16.84	−ve	$[C_{18}H_{16}O_8]^{-H}$, 197.0435, 161.0232, 135.0441
19	Tinosporide	$C_{20}H_{22}O_7$	374.1366	419.1318	19.62	−ve	$[C_{20}H_{22}O_7]^{+HCOO}$, 195.0635, 193.0486, 181.0497
20	N-feruloyltyramine	$C_{18}H_{19}NO_4$	313.1314	314.1398 312.1210	19.70 19.76	+ve −ve	$[C_{18}H_{19}NO_4]^{+H}$, 220.0975, 177.0544, 149.0591, 145.0280, 121.0644, 103.0540 $[C_{18}H_{19}NO_4]^{-H}$, 296.0899, 190.0489, 178.0491, 148.0517, 135.0442, 134.0366

(Continues)

TABLE 1 (Continued)

Peak no.	Component name	Formula	Neutral mass (Da)	Observed m/z	RT (min)	Mode	Fragments (m/z)
21	Tinocordiside	$C_{21}H_{32}O_7$	396.2148	395.2046	20.92	−ve	$[C_{21}H_{32}O_7]^{-H}$, 178.0492
22	Withanoside VIII	$C_{46}H_{72}O_{20}$	944.4617	967.4547 989.4631	21.19 21.22	+ve −ve	$[C_{46}H_{72}O_{20}]^{+Na}$, 665.3919, 485.3243, 179.0537 $[C_{46}H_{72}O_{20}]^{+HCOO}$, 621.3630, 459.3102, 423.2886, 405.2780, 287.1996, 157.1002
23	Tanegoside C	$C_{27}H_{36}O_{13}$	568.2156	567.2087	21.95	−ve	$[C_{27}H_{36}O_{13}]^{-H}$, 179.0550
24	Quercetin	$C_{15}H_{10}O_7$	302.0427	303.0497 301.0316	21.98 22.09	+ve −ve	$[C_{15}H_{10}O_7]^{+H}$, 181.0502 $[C_{15}H_{10}O_7]^{-H}$, 151.0440
25	Luteolin	$C_{15}H_{10}O_6$	286.0477	287.0551 285.0371	22.21 22.31	+ve −ve	$[C_{15}H_{10}O_6]^{+H}$, 269.0432, 161.0225, 153.0176, 135.0431 $[C_{15}H_{10}O_6]^{-H}$, 151.0020, 133.0284, 132.0212, 107.0137
26	Withanoside IV	$C_{40}H_{62}O_{15}$	782.4089	783.4173 827.4129	26.95 26.97	+ve −ve	$[C_{40}H_{62}O_{15}]^{+H}$, 621.3622, 459.3101, 423.2887, 405.2780, 317.1748, 157.1002 $[C_{40}H_{62}O_{15}]^{+HCOO}$, 533.2754, 487.2683, 451.2461, 221.0640, 179.0543
27	3-HDH-withanolide F	$C_{28}H_{40}O_7$	488.2774	489.2858 533.2758	27.57 27.61	+ve −ve	$[C_{28}H_{40}O_7]^{+H}$, 453.2624, 435.2525, 317.1748, 299.1640 $[C_{28}H_{40}O_7]^{+HCOO}$, 436.2229
28	Viscosalactone B	$C_{28}H_{40}O_7$	488.2774	489.2861 533.2761	28.12 28.15	+ve −ve	$[C_{28}H_{40}O_7]^{+H}$, 359.2213, 317.1747, 299.1642 $[C_{28}H_{40}O_7]^{+HCOO}$, 469.2576, 329.2099
29	Kaempferol	$C_{15}H_{10}O_6$	286.0477	287.0548 285.0371	28.47 28.59	+ve −ve	$[C_{15}H_{10}O_6]^{+H}$, 229.0480, 153.0175, 147.0428 $[C_{15}H_{10}O_6]^{-H}$
30	Withanolide E	$C_{28}H_{38}O_7$	486.2618	531.2571	29.07	−ve	$[C_{28}H_{38}O_7]^{+HCOO}$, 195.0685
31	Physagulin D	$C_{34}H_{52}O_{10}$	620.3561	665.3573	29.87	−ve	$[C_{34}H_{52}O_{10}]^{+HCOO}$, 179.0539
32	2,3-didehydrosomnifericin	$C_{28}H_{40}O_7$	488.2774	489.2840	31.90	+ve	$[C_{28}H_{40}O_7]^{+H}$, 435.2529, 417.2407, 317.1743, 299.1632, 95.0485
33	3α,6α-epoxy-4β,5β,27-trihydroxy-1-oxowitha-24-enolide	$C_{28}H_{40}O_7$	488.2774	489.2840	32.24	+ve	$[C_{28}H_{40}O_7]^{+H}$, 435.2527, 317.1739, 299.1631, 187.1468, 133.1000
34	Coagulin Q	$C_{34}H_{52}O_{10}$	620.3561	665.3565	32.61	−ve	$[C_{34}H_{52}O_{10}]^{+HCOO}$, 171.1010, 137.0961
35	24,25-Dihydrowithanolide D	$C_{28}H_{40}O_6$	472.2825	473.2911	33.66	+ve	$[C_{28}H_{40}O_6]^{+H}$, 437.2679, 419.2559, 301.1809, 283.1692, 265.1585
36	2,3-dihydro-3β-O-sulfate withaferin A	$C_{28}H_{40}O_{10}S$	568.2342	569.2426 567.2277	35.36 35.66	+ve −ve	$[C_{28}H_{40}O_{10}S]^{+H}$, 471.2720, 397.1312, 379.1197, 317.1748, 299.1634, 147.1160, 123.1161 $[C_{28}H_{40}O_{10}S]^{-H}$, 301.1785, 96.9603
37	2,3-Dihydrowithaferin-A	$C_{28}H_{40}O_6$	472.2825	473.2893 517.2791	35.95 35.99	+ve −ve	$[C_{28}H_{40}O_6]^{+H}$, 437.2671, 343.2274, 325.2146, 301.1786, 283.1682, 121.0642 $[C_{28}H_{40}O_6]^{+HCOO}$, 405.2417
38	Withaferin A	$C_{28}H_{38}O_6$	470.2668	471.2762 515.2630	36.63 36.64	+ve −ve	$[C_{28}H_{38}O_6]^{+H}$, 435.2532, 281.1540 $[C_{28}H_{38}O_6]^{+HCOO}$, 436.2226
39	Quresimine A	$C_{29}H_{42}O_7$	502.2931	503.3017	38.22	+ve	$[C_{29}H_{42}O_7]^{+H}$, 441.2622, 313.1800, 255.1368, 121.0643
40	Cirsilineol	$C_{18}H_{16}O_7$	344.0896	345.0969	38.24	+ve	$[C_{18}H_{16}O_7]^{+H}$
41	Withanoside V	$C_{40}H_{62}O_{14}$	766.4140	767.4230 811.4182	41.53 41.54	+ve −ve	$[C_{40}H_{62}O_{14}]^{+H}$, 605.3667, 443.3150, 407.2935, 389.2821, 253.1938, 211.1470, 157.1002 $[C_{40}H_{62}O_{14}]^{+HCOO}$, 603.3540, 487.3418, 221.0640, 179.0543

(Continues)

TABLE 1 (Continued)

Peak no.	Component name	Formula	Neutral mass (Da)	Observed m/z	RT (min)	Mode	Fragments (m/z)
42	Withanone	$C_{28}H_{38}O_6$	470.2668	471.2723 515.2553	42.35 42.05	+ve −ve	$[C_{28}H_{38}O_6]^{+H}$ $[C_{28}H_{38}O_6]^{+HCOO}$
43	Cirsimaritin	$C_{17}H_{14}O_6$	314.0790	315.0862	44.05	+ve	$[C_{17}H_{14}O_6]^{+H}$, 299.0543, 282.0514, 271.0594, 197.0469, 181.0116, 153.0171, 136.0151, 118.0407
44	Methyl rosmarinate	$C_{19}H_{18}O_8$	374.1002	375.1068 373.0889	44.73 44.79	+ve −ve	$[C_{19}H_{18}O_8]^{+H}$, 359.0753, 197.0434, 163.0385 $[C_{19}H_{18}O_8]^{-H}$
45	12-deoxywithastramonolide	$C_{28}H_{38}O_6$	470.2668	515.2641	48.50	−ve	$[C_{28}H_{38}O_6]^{+HCOO}$, 451.2461, 325.1811, 223.1677
46	Ashwagandhanolide	$C_{56}H_{78}O_{12}S$	974.5214	975.5368 973.5207	49.60 49.60	+ve −ve	$[C_{56}H_{78}O_{12}S]^{+H}$, 767.3976, 515.2454, 435.2509, 369.2406, $[C_{56}H_{78}O_{12}S]^{-H}$, 503.2454, 501.2304
47	5-Hydroxy-7,8-dimethoxyflavone	$C_{17}H_{14}O_5$	298.0841	299.0917	50.77	+ve	$[C_{17}H_{14}O_5]^{+H}$, 283.0596, 267.0648, 255.0647, 197.0447, 136.0150
48	5-hydroxy-4′,6,7-trimethoxyflavone	$C_{18}H_{16}O_6$	328.0947	329.1021	51.63	+ve	$[C_{18}H_{16}O_6]^{+H}$, 299.0544, 285.0757, 270.0512, 152.0097, 121.0646
49	Withanolide G	$C_{28}H_{38}O_5$	454.2719	455.2804	51.75	+ve	$[C_{28}H_{38}O_5]^{+H}$, 281.1539, 157.1003, 155.0703
50	Dieugenol	$C_{20}H_{22}O_4$	326.1518	349.1408	54.88	+ve	$[C_{20}H_{22}O_4]^{+Na}$, 294.1247, 257.0800, 242.0565, 147.0799, 119.0486
51	Betulinic acid	$C_{30}H_{48}O_3$	456.3604	455.3503	60.15	−ve	$[C_{30}H_{48}O_3]^{-H}$
52	Ursolic acid	$C_{30}H_{48}O_3$	456.3604	501.3570	60.62	−ve	$[C_{30}H_{48}O_3]^{+HCOO}$, 407.3294, 251.2354

study the linear regression. The LOD and LOQ of each marker component were determined based on S/N. S/N ratio was confirmed by injecting six replicates of minimum concentration at which the component was reliably detected and quantitated. The intraday and interday precisions ($n = 6$), were evaluated by calculating the %RSD of the observed value. The analytical recovery was performed by spiking sample with the reference standards at known concentration 80, 100, and 120%. Recoveries at different levels were calculated by comparing accepted reference value and value obtained. The robustness of the method was determined by incorporating deliberate variations in the chromatographic conditions such as change of column and flow rate. The stability analysis was performed by exposing the formulation to different solvents, thermal, and photochemical conditions. For thermal degradation, batches were exposed to 60°C and 80°C for the different time intervals up to 24 h. Similarly, the formulation was subjected to different wavelengths, i.e. 257, 366 nm, and white light at different time intervals. Moreover, the solution stability of the formulation was tested in methanol and 0.5% methylcellulose solution at 0 h and after 24 h at different temperatures i.e. room temperature (RT) and 4°C.

2.3.2 | High performance thin layer chromatography

The method was validated for quantification of withanoside IV, withaferin A, magnoflorine, palmatine, rosmarinic acid, and ursolic acid in CNT samples. Linearity was performed by plotting calibration curve similar to RP-HPLC. The LOD and LOQ were calculated by using the values of slopes and intercepts of the calibration curve. The intraday and interday precisions ($n = 9$) were evaluated by calculating %RSD at three different concentrations. The recovery of the method was evaluated using the standard addition method. The analysis was performed in triplicates at 80, 100, and 120% i.e. $n = 9$ by adding known quantities of reference standards to the CNT formulation.

2.4 | Quantitative analysis of Coronil samples

To assure the unwavering reliability of the created and approved RP-HPLC-PDA strategy, quantitative investigation of magnoflorine, rosmarinic acid, palmatine, withanoside IV, withaferin A, and withanoside V was done on
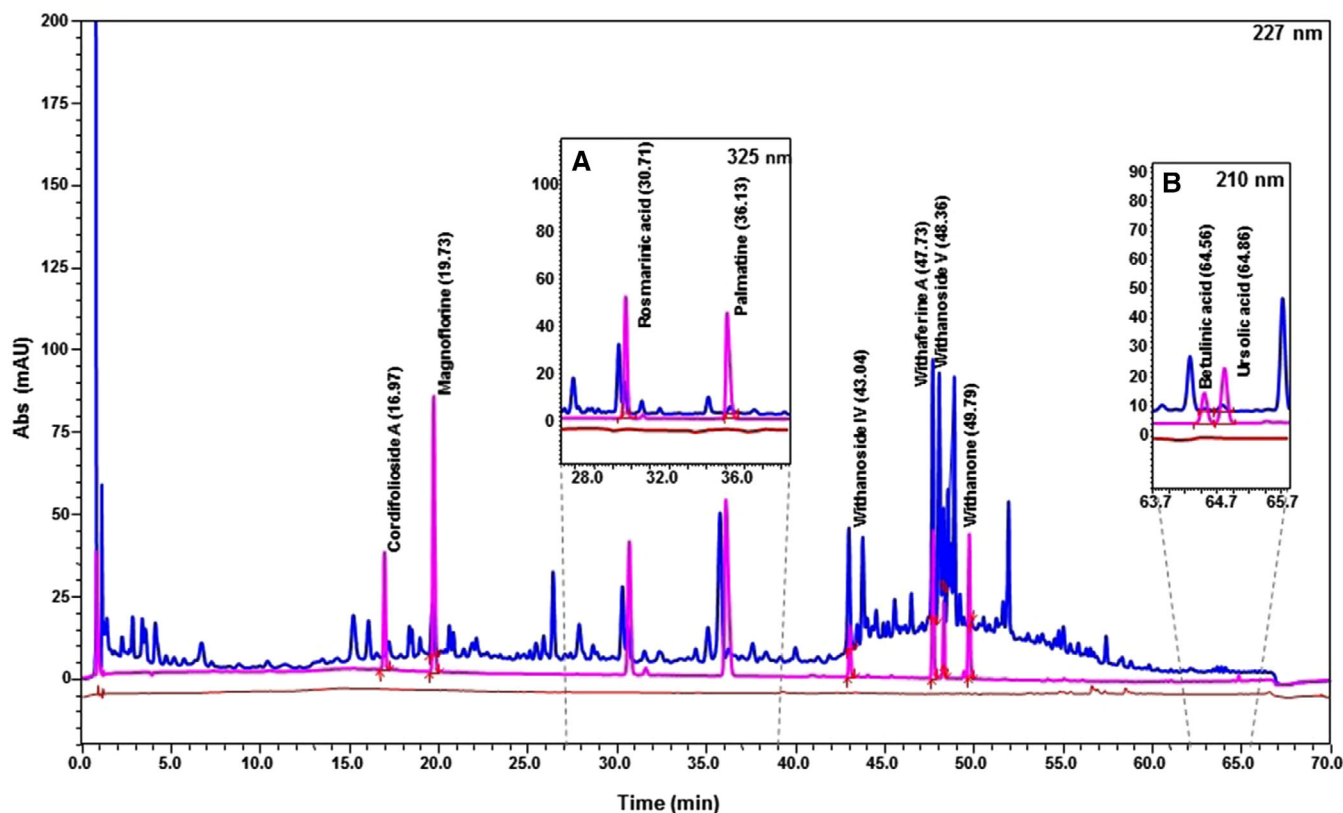
FIGURE 2 Overlap of RP-HPLC-PDA chromatogram for Coronil. Sample (blue lines) was compared using mix reference standard (pink lines) and sample blank (red lines). Cordifolioside A (RT:16.97), magnoflorine (RT:19.73), withanoside IV (RT:43.04), withaferin A (RT:47.73), withanoside V (RT:48.36), and withanone (RT:49.79) were quantified at 227 nm. Inset (A), rosmarinic acid (RT:30.71) and palmatine (RT:36.13) were quantified at 325 nm. Inset (B), betulinic acid (RT:64.56) and ursolic acid (RT:64.86) were quantified at 210 nm. RT is retention time

15 batches of CNT. The quantitative analysis was carried out by comparing the area under the curve of the analyte. For HPTLC, the concentration of withanoside IV, withaferin A, magnoflorine, palmatine, rosmarinic acid, and ursolic acid were determined by applying the samples (2–4 μL) along with the reference standards. The quantity of the markers was calculated using the regression equation obtained from the standard calibration curves.

2.5 | Data analysis

Statistical analyses were performed using Graph Pad Prism 7.0 (Graph pad Software, San Diego, CA, USA). Characterization of the marker analytes was performed using Unifi software Waters Corporation (MA, USA). RP-HPLC-PDA analysis was performed on LabSolutions (Shimadzu, Japan). HPTLC studies were performed using winCATS software (CAMAG, Muttenz, Switzerland). FTIR analysis was performed on MicroLab software (Agilent, Malasiya).

3 | RESULTS AND DISCUSSION

3.1 | Ultra high performance liquid chromatography–mass spectrometry coupled with quadrapole time of flight analysis characterized phytochemical markers in Coronil

A total of 52 compounds were recognized using UHPLC/MS-ToF, where 36 compounds were identified in the positive mode of ionization (Figure 1A, Table 1) and 39 compounds were identified in the negative mode of ionization (Figure 1B, Table 1). Twenty-three compounds were found to be common in both the ionization mode. The recognizable proof of compounds relied on the information of mass fragmentation patterns and accurate mass measurement of the targeted analytes. Further confirmation was achieved using an in-house spectral library and literature search (Figure S1, Table 1). Mass fragmentation pattern ascertained the presence of cordifolioside A, magnoflorine, palmitine in CNT, consequently, these markers were
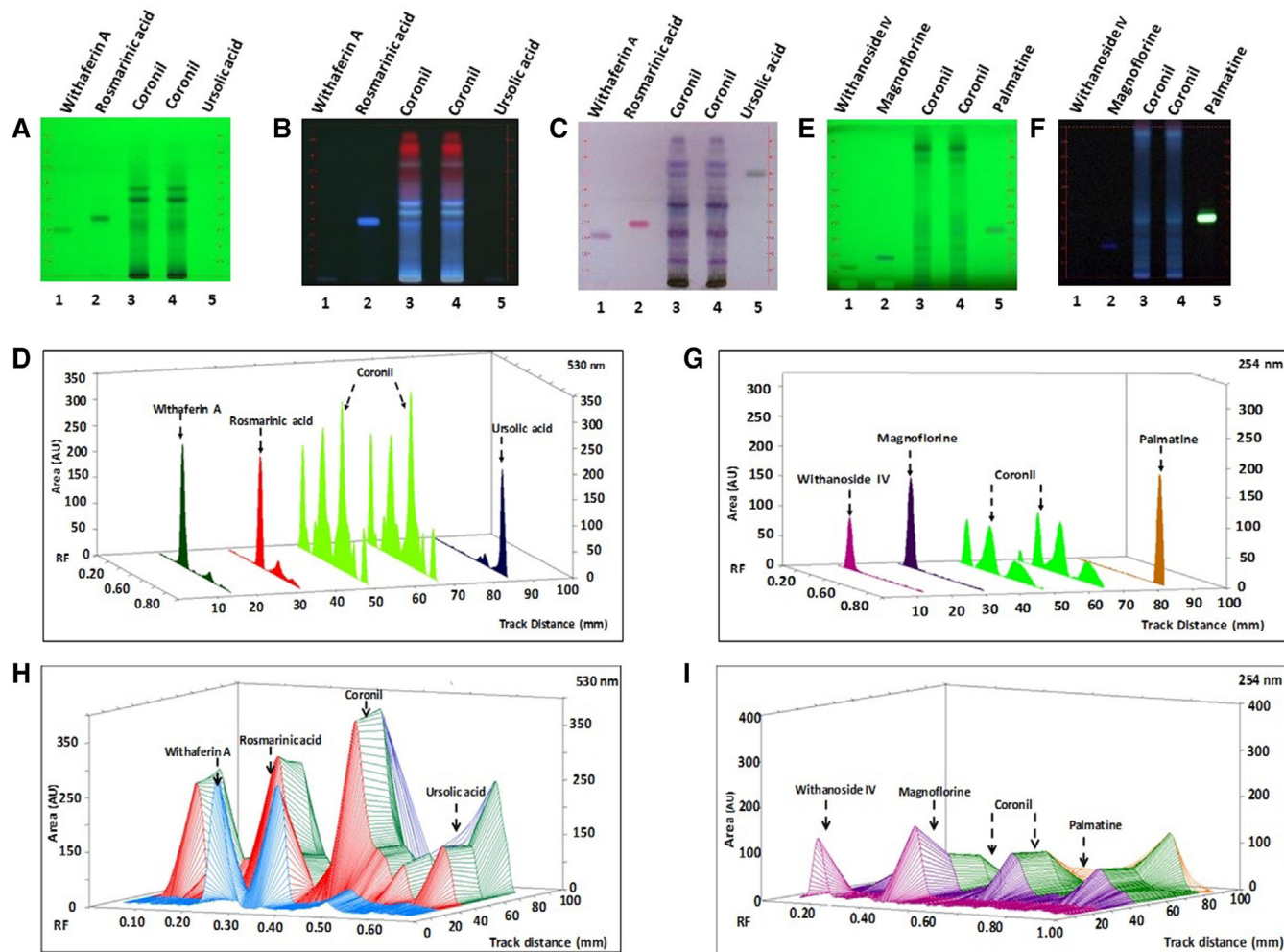
FIGURE 3 Chromatograms of Coronil in the High-Performance ThinLayer Chromatography (HPTLC) analysis. Chemical constituent analysis of CNT using HPTLC at A: 254 nm, B: 366 nm, C white light after derivatization with anisaldehyde-sulfuric acid. The spotting is shown as withaferin A (Track 1), rosmarinic acid (Track 2), Coronil (Track 3 and Track 4), ursolic acid (Track 5). Similarly, E: 254 and F: 366 showed withanoside IV (Track 1), magnoflorine (Track 2), Coronil (Track 3 and 4), palmatine (Track 5). D and H represent the 3D densitogram and hidden wire spectra of A, B, and C at 530 nm, G and I represent for E and F at 254 nm

chosen as the typical of *T. cordifolia*. MS-data distinguished ursolic acid, betulinic acid, and rosmarinic acid in the formulation, chosen as markers for *O. sanctum*. Furthermore, withaferin A, withanoside IV, withanoside V, and withanone were identified and chosen as the signature markers for *W. somnifera*. Thus, for RP-HPLC-PDA analysis, 10 marker analytes, cordifolioside A, magnoflorine, rosmarinic acid, palmatine, withanoside IV, withaferin A, withanoside V, withanone, betulinic, and ursolic acid were selected for standardization of CNT. Whereas, for HPTLC, six components viz., withanoside IV, withaferin A, magnoflorine, palmatine, ursolic acid, and rosmarinic acid were selected. The marker components were selected based on their established potential immunomodulatory activity and availability.

3.2 | Establishment and optimization of HPLC and high performance thin layer chromatography method

3.2.1 | HPLC

Chromatographic separation of 10 markers portrayed a big challenge, as these compounds have exceptionally wide as well as a close range of polarity index. The aim was to separate the targeted components with a compatible solvent system, gradient elution was therefore carried out so as to ensure that the elution of all the compounds was completed within a short time. Both reverse phase and normal phase were also tried but due to the prominence of polar moieties, reverse phase chromatography

TABLE 2 Validation parameters (RP-HPLC) of cordifolioside A, magnoflorine, rosmarinic acid, palmatine, withanoside IV, withanoside V, withanone, betulinic acid, and ursolic acid in Coronil

Parameters		Acceptance criteria	Results obtained									
			Cordifolioside A	Magnoflorine	Rosmarinic acid	Palmatine	Withanoside IV	Withaferine A	Withanoside V	Withanone	Betulinic acid	Ursolic acid
System suitability		%RSD area NMT-2	1.43	0.41	1.67	1.09	1.75	1.80	0.58	1.29	1.28	0.58
		Tailing factor NMT-2	0.990	1.250	1.020	1.64	0.970	1.020	1.103	0.978	0.989	0.978
		Theoretical plates NLT-5000	84 757	119 232	163 278	123 858	737 150	1042 818	1621 395	971 626	1908 232	1897 460
Specificity		No interference at retention time when compared to blank										
		Peak purity NLT-0. 980	0.997	0.990	0.987	0.991	0.994	0.985	0.986	0.982	0.998	0.983
Linearity		Correlation coefficient NLT-0.999	0.9997	0.9997	0.9997	0.9997	0.9997	0.9996	0.9991	0.9996	0.9999	0.9997
		Range (µg/g)	20–2000	5–2000	20–2000	20–2000	40–2000	20–2000	20–2000	20-2000	40-2000	40-2000
Precision	Intraday	%RSD NMT-5	BLQ	0.54	2.90	3.01	0.82	0.51	2.93	BLQ	BLQ	BLQ
	Interday	%RSD NMT-5	BLQ	0.78	0.86	1.69	0.79	0.98	1.14	BLQ	BLQ	BLQ
Mean average recovery (%)		90–110	95.25	100.1	99.79	94.99	94.80	95.39	97.61	93.94	96.56	96.8
Robustness	Column n = 12	%RSD NMT-20	BLQ	3.56	9.23	16.07	10.58	8.09	9.31	BLQ	BLQ	BLQ
	Flow rate n = 18	%RSD NMT-20	BLQ	4.05	3.29	13.31	13.17	11.83	13.38	BLQ	BLQ	BLQ
LOD, n = 6		%RSD of area NMT-33	3.59	1.78	1.29	0.76	1.60	2.01	2.86	5.41	8.53	2.68
		LOD (µg/g)	0.5	0.1	0.5	0.5	1.0	0.5	0.5	0.5	1.0	0.5
LOQ, n = 6		%RSD of area NMT-10	1.63	2.65	1.59	2.58	1.23	2.35	3.77	1.10	2.23	2.29
		LOQ (µg/g)	1.0	0.25	1.0	1.0	2.0	1.0	1.0	1.0	2.0	2.0

BLQ: Below limit of quantification; NLT: Not less than; NMT: Not more than.

TABLE 3 Validation parameters of high performance-TLC (HPTLC) for withanoside IV, withaferin A, magnoflorine, palmatine, rosmarinic acid and ursolic acid in Coronil

Parameters		Withanoside IV	Withaferin A	Magnoflorine	Palmatine	Rosmarinic acid	Ursolic acid
Retention factor (*Rf*)		0.25	0.38	0.21	0.55	0.32	0.66
Linearity	Correlation coefficient (NLT 0.99)	0.997	0.999	0.999	0.999	0.999	0.999
	Range (μg/ml)	200−600	600−1400	40−100	5−25	100-350	200-800
LOD (μg/g)		1.73	0.87	8.81	0.03	0.10	0.51
LOQ (μg/g)		5.26	2.63	26.71	0.10	0.31	1.53
Mean average recovery (90–110%)		98.89	93.91	99.43	96.91	96.73	95.64
Intraday precision (RSD%) NMT 2		0.94	1.04	0.97	0.83	0.95	1.24
Interday precision (RSD%) NMT 2		0.80	0.94	1.75	1.01	0.92	0.85

NMT: Not more than, NLT: Not less than.

was found to be the best solution for separation of the targeted analytes. After several trials of mobile phase and column optimization, the aforementioned method in the above section, effectively ensured that the needed separation of the targeted analytes was with acceptable peak shape and resolved between the peaks (Figure 2). Flow rates between 0.5 and 1 mL/min were tried for the current study. A flow rate of 0.7 mL/min gave reasonable separation of the compounds with high theoretical plates. Choice of the wavelength was quite difficult as all these compounds have different structures, distinctive spectra, and molar absorptivity. For that purpose, the chromatographic detection of the analytes was performed using a PDA detector which scans the entire spectrum (190 to 800 nm) simultaneously. Absorption maxima for cordifolioside A, magnoflorine, withanoside IV, withaferin A, withanoside V, and withanone was found at 227 nm. For rosmarinic acid and palmatine at 325 nm and for betulinic acid and ursolic acid the same was observed at 210 nm. The overlaid chromatograms of standard and sample depicted similar retention time confirming the targeted molecule, which was used for calculating the amount of active moieties in CNT. Thus, from the optimized RP-HPLC it is evident that targeted anaytes in CNT are well separated and their quantification can be carried out with adequate precision.

3.2.2 | High performance thin layer chromatography

Optimization indeed is a prime step of method development [19]. For optimizing the mobile phase, various combinations of organic solvents were tried such as hexane:ethyl acetate (60:40, 70:30, 80:20, 90:10), ethyl acetate:acetic acid:formic acid:water:methanol (10:1.1:1.1:2.6:1, 10:1.1:1.1:2.3:1), and toluene:ethyl

acetate:formic acid (16:24:2, 9.6:0.4:0.1). Finally, toluene:ethyl acetate:formic acid (5:5:1) was selected for withaferin A, rosmarinic acid, and ursolic acid with *Rf* (retention factor) value 0.33, 0.40, and 0.70, respectively. Ethyl acetate:formic acid:acetic acid:water (10:1.1:1.1:2.6) was chosen for withanoside IV, magnoflorine, and palmatine with *Rf* value 0.14, 0.19, and 0.34, respectively. The chromatographic scanning was performed at wavelength*s* 530 and 254 nm (Figure 3). Due to lack of the chromophore moieties, triterpenoids show low UV absorptivity. Derivatization with the chemical reagents is used to detect these classes of compounds in the visible region. In our investigation, for the fingerprinting and quantitative analysis of usrolic acid, derivatization was employed using anisaldehyde sulphuric acid. Post derivatization results revealed a bright purple-colored band (*Rf* 0.70), corresponding to ursolic acid at 530 nm indicating the specificity of the developed method.

3.3 | Validation of the developed HPLC and high performance thin layer chromatography methods

The RP-HPLC-PDA and HPTLC methods were validated in terms of linearity, limits of quantification, detection, accuracy, and precision. Determination of system suitability, specificity, and robustness was additionally done for RP-HPLC-PDA (Tables 2 and 3).

3.3.1 | Specificity, limits of detection and quantification

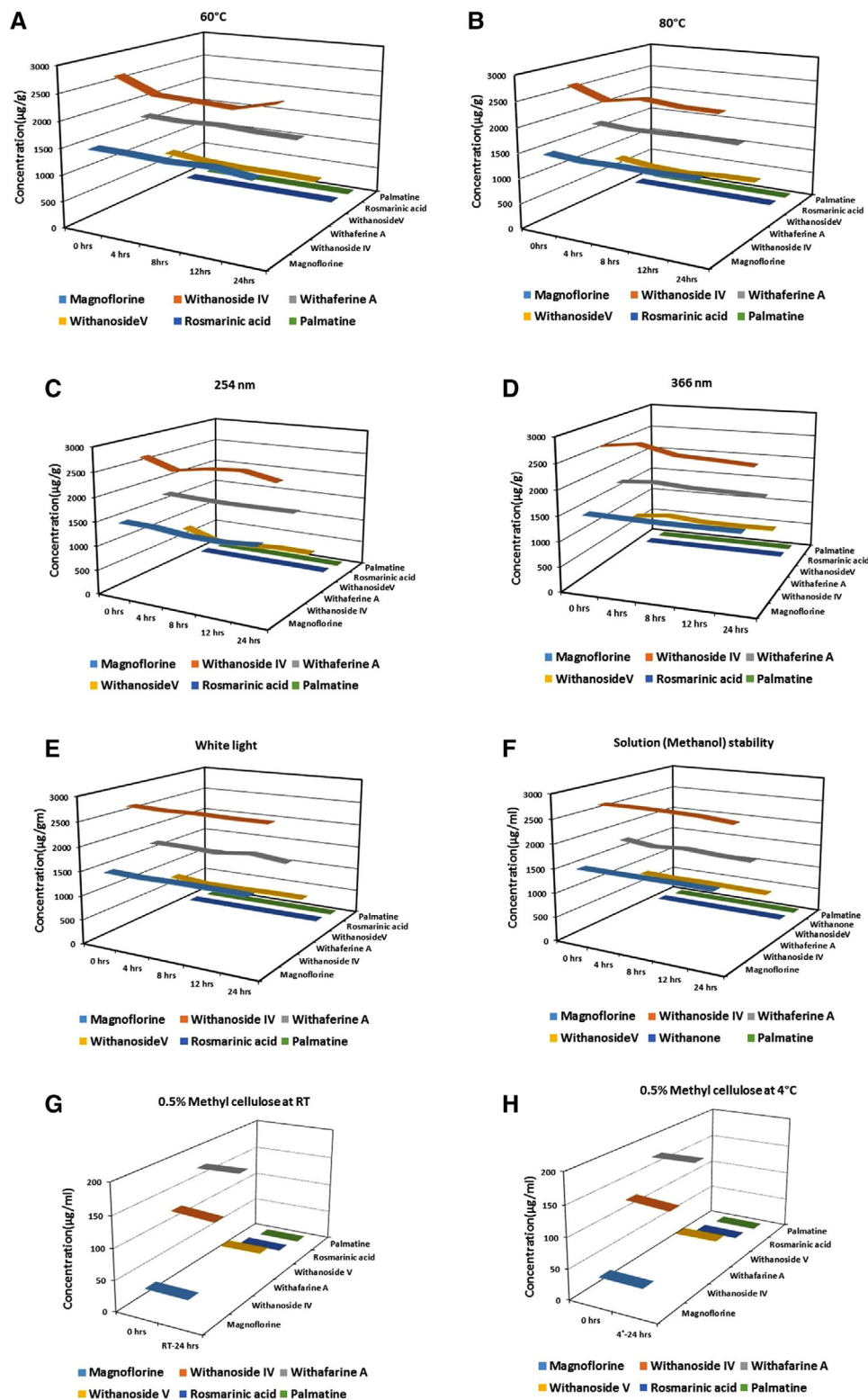For RP-HPLC-PDA the specificity of the method was monitored by comparing the chromatograms of solvent blank,

FIGURE 4 Stability analysis of Coronil at different conditions for the marker compounds magnoflorine, withanoside IV, withaferin A, withanoside V, rosmarinic acid, and palmatine in the batches (#ACNT 0194, 009 and 460). (A) 60°C, (B) 80°C, (C) 254 nm, (D) 366 nm, (E) white light, (F) in methanol at 0, 4, 8, 12, and 24 h, respectively. (G and H) 0.5% methyl cellulose suspension at 0 h, room temperature (RT), and for 24 h and 4°C. The concentration of the targeted analytes was analyzed using RP-HPLC-PDA
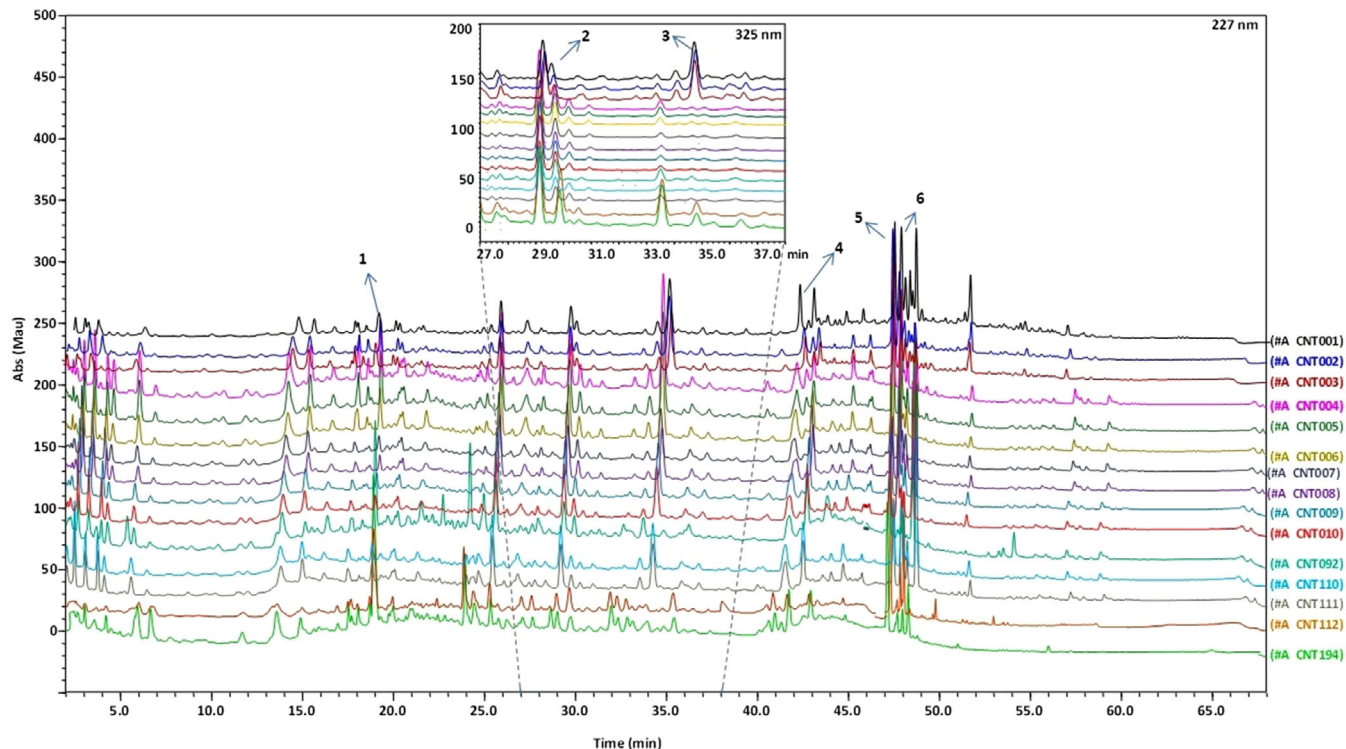
FIGURE 5 Comparative RP-HPLC-PDA profile of 15 Coronil batches (#ACNT 001 to 010, 092, 110 to 112, and 194). The profile ascertained the presence of targeted analytes in the above batches designated by peak numbers: (1) magnoflorine, (2) rosmarinic acid, (3) palmatine, (4) withanoside IV, (5) withaferin A, and (6) withanoside V

standard mix, and sample matrix. In solvent blank chromatogram, no peaks were detected close to the retention time of the selected marker components. Moreover, the peak purity of all the targeted analytes was found to be >0.980 confirming that there is no interference of the solvent, diluent, and other close eluting compounds at the RT of the marker components (Figure 2). The obtained LOD and LOQ values for cordifolioside A, rosmarinic acid, palmatine, withaferin A, withanoside V, and withanone were 0.5 and 1.0 µg/g, respectively. Similarly, for withanoside IV and betulinic acid those were 1.0 and 2.0 µg/g, whereas, for magnoflorine 0.1 and 0.25 µg/g and for ursolic acid it was 0.5 and 2.0 µg/g (Table 2). For HPTLC, the LOD and LOQ values were found to be (1.73 and 5.26 µg/g), (0.87 and 2.63 µg/g), (8.81 and 26.71 µg/g), (0.03 and 0.10 µg/g), (0.10 and 0.31 µg/g), (0.51 and 1.53 µg/g) for withanoside IV, withaferin A, magnoflorine, palmatine, rosmarinic acid, and ursolic acid, respectively (Table 3). The observed results were found to be within the acceptance criteria (NMT 33% and NMT 10% for LOD and LOQ, respectively). For reported RP-HPLC and HPTLC methods, the value obtained for LOD and LOQ (Tables 2 and 3, respectively) indicated that the method is sensitive to detect and quantify the target analytes at very low level.

3.3.2 | Linearity and range

For RP-HPLC-PDA and HPTLC, the calibration curve exhibited a good linear relationship for all compounds with correlation coefficient ranging from 0.997 to 0.999 (Tables 2 and 3). Thus, indicating that the proposed analytical methods are linear and suitable for the quantification of the targeted analytes in CNT. The results of the regression equation are depicted in Figures S2 and S3. Based on LOD, LOQ, and linearity determinations for RP-HPLC, the lowest working range was found to be 5 µg/g for magnoflorine, 20 µg/g for cordifolioside A, rosmarinic acid, palmatine, withaferin A, withanoside V, withanone and 40 µg/g for withanoside IV, betulinic acid and ursolic acid. Whereas, higher range for all the targeted molecules was 20 00 µg/g. The working range of HPTLC was 200–600 µg/mL for withanoside IV, 600–1400 µg/mL for withaferin A, 40–100 µg/mL for magnoflorine, 5–25 µg/mL for palmatine, 100–350 µg/mL for rosmarinic
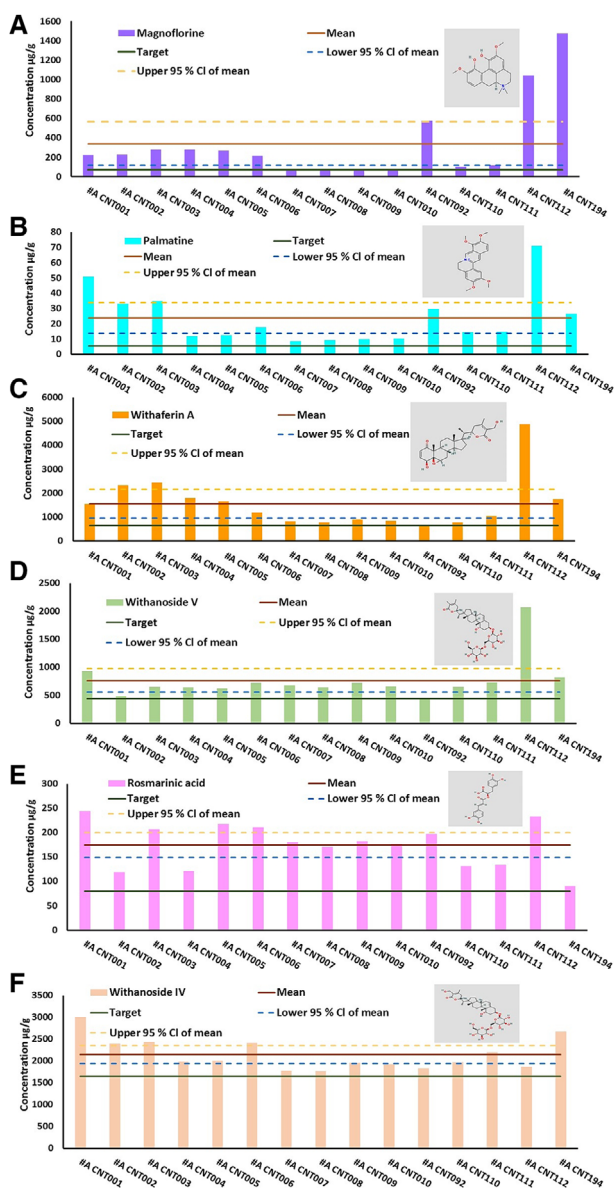
FIGURE 6 Content uniformity performed using RP-HPLC-PDA analysis in 15 different batches of Coronil, (#ACNT 001 to 010, 092, 110 to 112, and 194) . (A) magnoflorine, (B) palmatine, (C) withaferin A, (D) withanoside V, (E) rosmarinic acid, and (F) withanoside IV. Chemical structure of analytes have been sourced from www.pubchem.com (accessed on April 22, 2021)

acid, and 200–800 µg/mL for ursolic acid (Tables 2 and 3), indicating that these methods are applicable for a wide concentration range of active molecules in CNT.

3.3.3 | Accuracy

Accuracy refers to the closeness of the agreement between the true value and obtained results [18]. The accuracy of all the targeted signature analytes, by both the analytical methods was evaluated by the standard addition method.

The recoveries of the marker compounds at aforementioned concentrations are ranged from 93 to 100% (Tables 2 and 3). The results proved that the established RP-HPLC-PDA and HPTLC method is accurate for the simultaneous determination of phytocomponents in CNT.

3.3.4 | Precision

The precision of the developed RP-HPLC-PDA method was verified by intraday and interday ($n = 6$) analysis. %RSD was computed and was within the permissible criteria of ⁵5% for magnoflorine, rosmarinic acid, palmatine, withanoside IV, withaferin A, and withanoside V, confirming that the method was sufficiently precise. Whereas, cordifolioside A, withanone, betulinic acid, and ursolic acid, were found below the quantification limit (Table 2). The HPTLC method was also found to be precise (Table 3), with repeatability and intermediate precision within the acceptance criteria of ⁵2%.

3.3.5 | Robustness and stability analysis

The robustness of the analytical method should confirm the reliability of analysis concerning deliberate variations in the parameters. Variations in terms of column and flow rate did not produce any significant effect on the measured values. The %RSD of the 12 determinations, for the change in columns (lot number 20A00104 and 20A00105) ($n = 12$) and 18 determinations with change in flow rate from 0.665 to 0.7 mL/min and 0.735 mL/min ($n = 18$) were found to be within the prescribed limits (Table 2), indicating the robustness of the method.

Stability was performed under different conditions for 24 h to check the quality of the product during analysis and storage. Figure 4 shows the 3D graphs for the stability analysis. The targeted analytes (Z-axis) were plotted against concentration (Y-axis) at different time intervals (X-axis) with variation in temperature and light conditions. A methanolic solution of CNT (up to 50 mg/mL) was found to be stable for 24 h. Furthermore, the results also indicated that the CNT formulation of 100 mg/mL in 0.5% methylcellulose is stable for 24 h.

3.4 | Validated HPLC and high performance thin layer chromatography methods simultaneously quantified targeted analytes in coronil

The developed and validated analytical method was successfully used for the simultaneous determination of
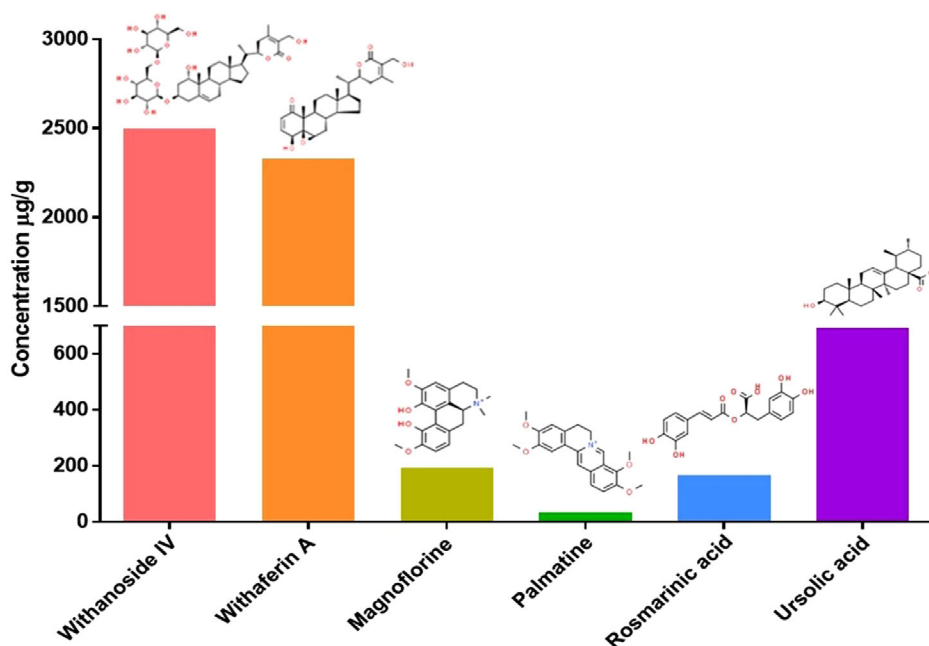
FIGURE 7 Quantitative analysis of targeted marker analytes; withanoside IV, withaferin A, magnoflorine, palmatine, rosmarinic acid, and ursolic acid using high-performance thin layer chromatography (HPTLC) method in batch (#ACNT 002) of Coronil. Chemical structure of analytes have been sourced from www.pubchem.com (accessed on April 22, 2021)
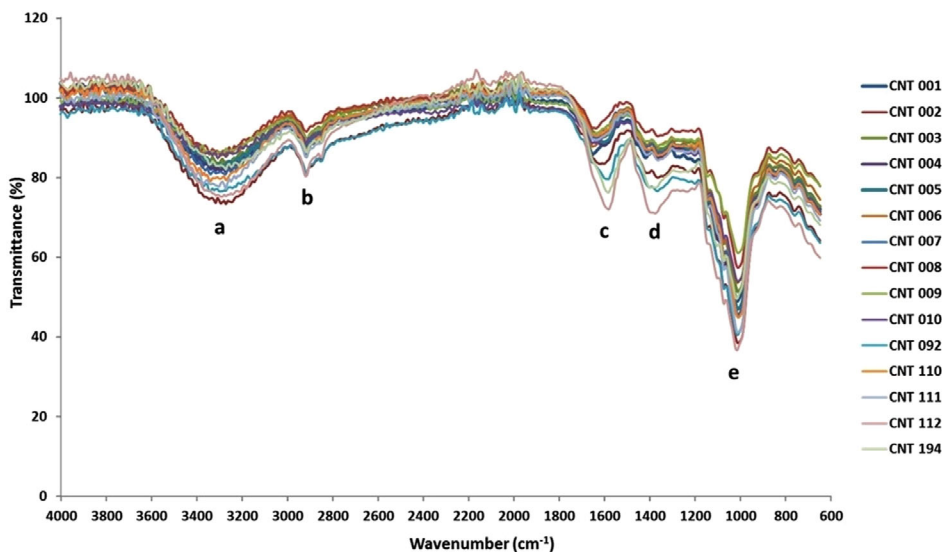

FIGURE 8 FTIR spectroscopy for the content uniformity analysis of 15 different batches of Coronil, (#ACNT 001 to 010, 092, 110 to 112, and 194). Where (a) is the peak corresponding to −O−H stretching, (b) C−H stretching, (c) N−O stretching, and C=N, (d) C−H bending, (e) C−C stretching, C−O, and/or C−N

marker components in 15 batches of CNT on RP-HPLC (Figure 5). It was observed that the concentrations of cordifolioside A, withanone, betulinic acid, and ursolic acid were below the limit of quantification (Figure 6). Accumulation of secondary metabolites in the plant material is often influenced by several factors; the most important of them are seasonal and geographical. Thus, it is evident

that the intricacies of herbal formulations demand a multimarker standardization approach because the phytochemicals ought to vary due to different external and internal factors. The developed and validated HPTLC method for the simultaneous estimation of six marker components was further applied to determine the content of biomarkers in CNT. For HPTLC, the column bar graph was

plotted which depicts the quantity of each targeted analyte (Figure 7). The results indicated that the proposed HPTLC strategy is pertinent for the analysis of the aforementioned analytes in the CNT formulation.

3.5 | Fourier transform infrared spectroscopy analysis of the content uniformity in 15 Coronil batches

In recent years, FTIR has emerged as a cost-effective analytical tool for verifying batch-to-batch consistency of the formulation [20]. Distinctive spectral pattern was observed during FTIR analysis of CNT indicating the presence of mixed functional groups like $O-H$ stretching ($3295\ cm^{-1}$), $C-H$ bending ($2922\ cm^{-1}$), $N-O$ and/or $C=N$ ($1580\ cm^{-1}$), C-H bending ($1379\ cm^{-1}$), $C-C$ stretching, and/or $C-O$ and/or $C-N$ ($1013\ cm^{-1}$) group (Figure 8). The results obtained provide information about the spectral behavior and content uniformity which can be further utilized for reaffirming the consistency of Coronil batches.

4 | CONCLUDING REMARKS

In this study, 52 phytometabolites were identified in Coronil by a rapid UPLC/MS-ToF technique, ensued by simultaneous estimation of the selected ten and six markers using RP-HPLC-PDA and HPTLC, respectively. To establish consistency of validated method, concurrent determination of magnoflorine, rosmarinic acid, palmatine, withanoside IV, withaferin A, and withanoside V in 15 different batches of Coronil was studied by RP-HPLC. Content uniformity was also established by FTIR spectroscopy fingerprinting in the same Coronil batches. The results suggest that method development is significant to ensure batch-to-batch consistency in terms of quality. Developed methods can be utilized by herbal manufacturers as quality control strategy for herbal extracts and formulations containing similar herbs such as *Withania somnifera*, *Ocimum sanctum*, and *Tinospora cordifolia* for their reproducible pharmacological effects.

CONFLICT OF INTEREST
The test articles were provided by Divya Pharmacy, Haridwar, Uttarakhand, India. Acharya Balkrishna is an honorary trustee in Divya Yog Mandir Trust, that governs Divya Pharmacy, Haridwar. In addition, he holds an honorary managerial position in Patanjali Ayurved Ltd., Haridwar, India. Other than providing the test formulations, Divya Pharmacy was not involved in any aspect of research reported in this study. All other authors have declared no conflict of interest.

AUTHOR CONTRIBUTIONS
Acharya Balkrishna provided broad direction for the study, identified the test formulations, generated resources, and gave final approval for the manuscript. **Meenu Tomer** performed the RP-HPLC-PDA analysis and investigations. **Sudeep Verma** performed the UPLC/QToF MS analysis and investigations. **Monali Joshi** performed the HPTLC analysis and investigations. **Priyanka Sharma** performed data curing, and wrote the manuscript. **Jyotish Srivastava** supervised analytical chemistry experiments and reviewed the manuscript. **Anurag Varshney** conceptualized and supervised the overall studies, generated resources, critically reviewed, and finally approved the manuscript

ORCID
Anurag Varshney https://orcid.org/0000-0001-8509-0882

REFERENCES
1. Pappa S, Ntella V, Giannakas T, Giannakoulis VG, Papoutsi E, Katsaounou P. Prevalence of depression, anxiety, and insomnia among healthcare workers during the COVID-19 pandemic: a systematic review and meta-analysis. Brain Behav Immun. 2020;88:901–7.
2. Chen J, Lu H, Melino G, Boccia S, Piacentini M, Ricciardi W, Wang Y, Shi Y, Zhu T. COVID-19 infection: the China and Italy perspectives. Cell Death Dis. 2020;11:438.
3. Vellingiri B, Jayaramayya K, Iyer M, Narayanasamy A, Govindasamy V, Giridharan B, Ganesan S, Venugopal A, Venkatesan D, Ganesan H, Rajagopalan K, Rahman PKSM,

Cho S-G, Kumar NS, Subramaniam MD. COVID-19: a promising cure for the global panic. Sci Total Environ. 2020;725:138277.

4. Gautam S, Gautam A, Chhetri S, Bhattarai U. Immunity against covid-19: potential role of ayush kwath. J Ayurveda Integr Med. 2020:1–8.

5. Sharma U, Bala M, Kumar N, Singh B, Munshi RK, Bhalerao S. Immunomodulatory active compounds from Tinospora cordifolia. J Ethnopharmacol. 2012;141:918–26.

6. Jadhav V. Anti- SARS-CoV-2 main protease complex (Mpro) activity of Palmatine. Res Sq. 2020;431801:1–19.

7. Rastogi S, Kalra A, Gupta V, Khan F, Lal RK, Tripathi AK, Parameswaran S, Gopalakrishnan C, Ramaswamy G, Shasany AK. Unravelling the genome of holy basil: an "incomparable" "elixir of life" of traditional Indian medicine. BMC Genomics. 2015;16:413.

8. Ghoke SS, Sood R, Kumar N, Pateriya AK, Bhatia S, Mishra A, Dixit R, Singh VK, Desai DN, Kulkarni DD, Dimri U, Singh VP. Evaluation of antiviral activity of Ocimum sanctum and Acacia arabica leaves extracts against H9N2 virus using embryonated chicken egg model. BMC Complement Altern Med. 2018;18:174.

9. Wen C-C, Kuo Y-H, Jan J-T, Liang P-H, Wang S-Y, Liu H-G, Lee C-K, Chang S-T, Kuo C-J, Lee S-S, Hou C-C, Hsiao P-W, Chien S-C, Shyur L-F, Yang N-S. Specific plant terpenoids and lignoids possess potent antiviral activities against severe acute respiratory syndrome coronavirus. J Med Chem. 2007;50:4087–95.

10. Singh DP, Tripathi PK, Shalini T, Verma NK, Chandra V, Asha R. Phytochemical constituents and pharmacological activities of Ocimum sanctum (Tulsi): a review. J Pharm Res Clin Pract. 2012;2:118–26.

11. Tripathi MK, Singh P, Sharma S, Singh TP, Ethayathulla AS, Kaur P. Identification of bioactive molecule from Withania somnifera (Ashwagandha) as SARS-CoV-2 main protease inhibitor. J Biomol Struct Dyn. 2020;39:1–14.

12. Balkrishna A, Pokhrel S, Joshi MJ, Mulay VP, Haldar S, Varshney A. Withanone from *Withania somnifera* attenuates SARS-CoV-2 RBD and host ACE2 interactions to rescue spike protein induced pathologies in humanized zebrafish model. Drug Des Devel Ther. 2021;15:1111.

13. Balkrishna A, Pokhrel S, Varshney A. Tinocordiside from Tinospora cordifolia (giloy) may curb SARS-CoV-2 contagion by disrupting the electrostatic interactions between host ACE2 and viral s-protein receptor binding domain. Comb Chem High Throughput Screen. 2020;23:15.

14. Balkrishna A, Solleti SK, Verma S, Varshney A. Application of humanized zebrafish model in the suppression of SARS-CoV-2 spike protein induced pathology by tri-herbal medicine coronil via cytokine modulation. Molecules. 2020;25:5091.

15. Balkrishna A, Haldar S, Singh H, Roy P, Varshney A. Coronil, a tri-herbal formulation, attenuates spike-protein-mediated SARS-CoV-2 viral entry into human alveolar epithelial cells and pro-inflammatory cytokines production by inhibiting spike protein-ACE-2 interaction. J Inflamm Res. 2021;14:869–84.

16. Yuan H, Ma Q, Cui H, Liu G, Zhao X, Li W, Piao G. How can synergism of traditional medicines benefit from network pharmacology? Molecules. 2017;22:1135.

17. Wu L, Hao H, Wang G. LC/MS based tools and strategies on qualitative and quantitative analysis of herbal components in complex matrixes. Curr Drug Metab. 2012;13:1251–65.

18. International Conference on Harmonization (ICH-Q2 R1). *Validation of Analytical Procedures: Text and Methodology*. Geneva, Switzerland: ICH Secretariat; 2005.

19. Mattrey FT, Makarov AA, Regalado EL, Bernardoni F, Figus M, Hicks MB, Zheng J, Wang L, Schafer W, Antonucci V, Hamilton SE, Zawatzky K, Welch CJ. Current challenges and future prospects in chromatographic method development for pharmaceutical research. Trends Anal Chem. 2017;95:36–46.

20. Lawson G, Ogwu J, Tanna S. Quantitative screening of the pharmaceutical ingredient for the rapid identification of substandard and falsified medicines using reflectance infrared spectroscopy. PLoS One. 2018;13:e0202059.

SUPPORTING INFORMATION

Additional supporting information may be found in the online version of the article at the publisher's website.